From Fig. 2(a) it is seen, for example, that for $l_0 = 13$ the magnetization saturates in a field range which agrees quite well with the measurements. The calculations are not very sensitive to the value of l_0; for $l_0 = 10$ and $l_0 = 20$ one still obtains magnetization curves saturating in the desired field range. Of course, the magnitude of the magnetic moment varies strongly with l_0. Lacking an exact knowledge of the number of spherical particles present in the samples, it is not possible to make a decision on the most realistic value of l_0, a value which should be regarded as an average over all possible allowed orbital quantum numbers for particles of different size as present in the experiment.

The increase in the saturation magnetization as the temperature is lowered can be explained in two ways. It is possible that by the extrapolation procedure of Fig. 1(a) the almost linear but not yet saturated high field part of $M(H)$ also has been subtracted; on the other hand, it cannot be excluded that the eigenvibrations of the particles which destroy the spherical symmetry are frozen out, causing pure states with higher l values to be occupied.

It seems that orbital paramagnetism could play an important role in our experiments. It is conceivable that Kubo's arguments remain valid if the specimens do not fulfil the conditions for orbital paramagnetism, as in the case of Taupin's experiments[5] where thin lithium platelets were investigated.

We are grateful to Dr. A. P. van Gelder for many interesting discussions.

---

[1]H. Fröhlich, Physica (Utrecht) 4, 406 (1937).

[2]R. Kubo, J. Phys. Soc. Jap. 17, 975 (1962).

[3]L. P. Gorkov and G. M. Eliashberg, Zh. Eksp. Teor. Fiz. 48, 1407 (1965) [Sov. Phys. JETP 21, 940 (1965)].

[4]R. Denton, B. Mühlschlegel, and D. J. Scalapino, Phys. Rev. Lett. 26, 707 (1971).

[5]Ch. Taupin, J. Phys. Chem. Solids 28, 41 (1967).

[6]S. Kobayashi, T. Takahashi, and W. Sasaki, Phys. Lett. 33A, 429 (1970, and J. Phys. Soc. Jap. 31, 1442 (1971), and 32, 1234 (1972).

[7]R. Dupree and M. A. Smithard, J. Phys. C: Proc. Phys. Soc., London 5, 408 (1972); F. Meier and P. Wyder, Phys. Lett. 39A, 51 (1972); see also S. Strässler, M. J. Rice, and P. Wyder, Phys. Rev. B 6, 2575 (1972).

[8]The indium wire was supplied by N. V. Kaweki-Billiton, P. O. Box 38, Arnhem, The Netherlands. Purity: 99.9995%.

[9]H. R. Zeller and I. Giaever, Phys. Rev. 181, 789 (1969).

[10]J. H. P. Watson, Phys. Rev. B 2, 1282 (1970).

[11]We are indebted to Mr. Y. Tamminga, Universiteit van Amsterdam, for carrying out these measurements.

[12]A. H. Cooke, H. Meyer, W. P. Wolf, D. F. Evans, and R. E. Richards, Proc. Roy. Soc., Ser. A 225, 112 (1954).

[13]C. Kittel, Introduction to Solid State Physics (Wiley, New York, 1971), 4th ed., Chap. 7, p. 248, Table 1.

Kinematical Interpretation of Anomalous Thresholds

Yu-Chien Liu

Institute for Theoretical Physics, University of Nijmegen, Nijmegen, The Netherlands
(Received 21 November 1972)

It is observed that for a normal threshold $|\vec{q}|^2 = q_x^2 + q_y^2 + q_z^2 = 0$, for a triangular anomalous threshold $q_\perp^2 = q_x^2 + q_y^2 = 0$, and for a box anomalous threshold $q_y^2 = 0$, when scattering is taking place in the xz plane, with incident (or outgoing) particles moving along the z axis.

In attempting to derive dispersion relations for form factors[1,2] and scattering amplitudes[3] from perturbation theory, people have discovered the presence of anomalous thresholds in the physical sheet when the participating particles satisfy certain mass relations. It has been pointed out earlier[1] that all relevant intermediate particles must be put on the mass shell in order to produce these singularities; energy and momentum can still be conserved at each vertex, but with real energy and complex momentum.

Subsequently, Landau[4] proposed a method of locating the singularities of any given perturbative diagram. A Landau singularity is permitted if, in a reduced diagram, all intermediate particles are real (i.e., $q_i^2 + m_i^2 = 0$), and $\sum \alpha_i q_i = 0$ within a loop. The singularity will be present in the physical sheet if $\alpha_i \geq 0$ for all i; otherwise it

lies on an unphysical one. The triangle and box diagrams are special cases of the Landau equations.

Cutkosky[5] moved one step further in providing a rule to evaluate the discontinuity across the cut associated with a given Landau singularity. The prescription is to replace each propagator $(q_i^2 + m_i^2 - i\epsilon)^{-1}$ in a reduced diagram by $2\pi i \times \delta_p(q_i^2 + m_i^2)$,[6] which fulfills one of the Landau conditions one started with. On the other hand, the result is completely independent of the α_i, lucky in that it may be independent of the perturbation theory, while unlucky because it also yields no information about the Riemann-sheet structure of the amplitude for this singularity.

At the same time Mandelstam[7] attacked the problem with an analytic continuation of certain external masses in the ordinary unitarity equation. In practical cases,[8] Mandelstam's method reproduces what is contained in the Landau-Cutkosky theory, plus allowing a determination of the phase which is ambiguous in Cutkosky's

formula. What is surprising is, of course, that the two approaches should yield the same result.

That the anomalous thresholds emerge from an unphysical sheet into the physical one when the external mass increases from a tightly bound state to a loosely bound one (e.g., D, Σ, etc.), has called for a dynamical interpretation[9] of these singularities. There are also attempts[10] to promote the anomalous thresholds to near or even into the physical region to see the physical observable effects they may have.

In this note we report an observation made on the kinematical aspects of triangular and box anomalous thresholds. We base the discussion on Cutkosky's discontinuity formula, since it is the imaginary part of an amplitude which is more likely to yield all the singular structure a full amplitude can have. We illustrate the result with a particular box diagram shown in Fig. 1. A generalization to arbitrary masses shall be given later.

The Feynman amplitude for Fig. 1[11] (spin being neglected for simplicity) is

$$F(s, t) = \int d^4 q \{(q^2 + m_\Lambda^2)[(p_1 + k_1 - q)^2 + m_N^2][(-p_1 + q)^2 + m_\pi^2][(p_2 - q)^2 + m_\pi^2]\}^{-1} \tag{1}$$

multiplied by $i g_{\Sigma\Lambda\pi}^2 g_{NN\pi}^2/(2\pi)^4$. Let us work in the c.m. frame

$$p_1 = (0, 0, k, iE_\Sigma), \quad p_2 = (k\sin\theta, 0, k\cos\theta, iE_\Sigma),$$
$$k_1 = (0, 0, -k, iE_N), \quad k_2 = (-k\sin\theta, 0, -k\cos\theta, iE_N). \tag{2}$$

The discontinuity across the usually normal unitarity cut is obtained by replacing $(q^2 + m_\Lambda^2)^{-1}[(p_1 + k_1 - q)^2 + m_N^2]^{-1}$ with $(2\pi i)^2 \delta_p(q^2 + m_\Lambda^2)\delta_p[(p_1 + k_1 - q)^2 + m_N^2]$ in (1). These two δ functions give

$$q_0 = \tfrac{1}{2}(s + m_\Lambda^2 - m_N^2)s^{-1/2}, \tag{3}$$

and

$$|\vec{q}|^2 = \tfrac{1}{4}(s - s_n)(s - s_{n'})s^{-1}, \tag{4}$$

where $s_n = (m_\Lambda + m_N)^2$, $s_{n'} = (m_\Lambda - m_N)^2$, and s_n is the normal threshold.

The discontinuity across the triangular anomalous cut is given by further substitution[12] of $2\pi i \delta_p[(-p_1 + q)^2 + m_\pi^2]$ for $[(-p_1 + q)^2 + m_\pi^2]^{-1}$ in (1). In addition to (3) and (4), we have

$$kq_\parallel = \tfrac{1}{2}Q, \tag{5}$$

$$k^2 q_\perp^2 = -\tfrac{1}{4}m_\pi^2(s - s_t)(s - s_{t'})s^{-1}, \tag{6}$$

where $q_\parallel = q_z$, $q_\perp^2 = q_x^2 + q_y^2$, and

$$Q = 2E_\Sigma q_0 - m_\Sigma^2 - m_\Lambda^2 + m_\pi^2$$
$$= \tfrac{1}{2}[s^2 - (m_\Sigma^2 + m_\Lambda^2 + 2m_N^2)s + (m_\Sigma^2 - m_N^2)(m_\Lambda^2 - m_N^2)]s^{-1} + m_\pi^2, \tag{7}$$

$$(s_{t,t'}) = m_\Lambda^2 + m_N^2 + \tfrac{1}{2}M^2 \pm \tfrac{1}{2}(4m_\Lambda^2 m_\pi^2 - M^4)^{1/2}(4m_N^2 m_\pi^2 - m_\pi^4)^{1/2}m_\pi^{-2}. \tag{8}$$

In (8), $M^2 = m_\Sigma^2 - m_\Lambda^2 - m_\pi^2$, and s_t is the triangular anomalous threshold in the physical sheet; and here and hereafter, the upper choice for the ambiguous sign corresponds to the first choice of the double subscript.

Finally, the further replacement

$$[(p_2 - q)^2 + m_\pi^2] \to 2\pi i \, \delta_p[(p_2 - q)^2 + m_\pi^2]$$

in (1) yields the discontinuity across the anomalous box cut, as well as

$$kq_x = \tfrac{1}{2} Q(1 - \cos\theta)/\sin\theta, \tag{9}$$

$$k^2 q_y^2 = t(4m_\pi^2 - t)(s - s_b)(s - s_{b'})/16 s k^2 \sin^2\theta, \tag{10}$$

where

$$(s_b, s_{b'}) = (m_\Lambda^2 + m_N^2) + 2(4m_\pi^2 - t)^{-1}\{m_\pi^2 M^2 \pm [(4m_\pi^2 - t)m_\Lambda^2 - M^4]^{1/2}[(4m_\pi^2 - t)m_N^2 - m_\pi^4]^{1/2}\}. \tag{11}$$

s_b, which depends on t, is the box anomalous *threshold* in the physical sheet.

The kinematical interpretation of these *thresholds* is now clear; s_n is such that $|\vec{q}|^2 = q_x^2 + q_y^2 + q_z^2 = 0$, s_t corresponds to the condition that $q_\perp^2 = q_x^2 + q_y^2 = 0$, while s_b is the point at which $q_y^2 = 0$. We thus have a feeling that both s_t and s_b are a kind of threshold. Let us recall that we have a scattering occurring in the xz plane, with the initial particles moving in the z direction, and $t < 0$.

We also look at the deuteron problem (Fig. 2). With $d = (0, 0, k_d, \tfrac{1}{2}is^{1/2})$, $\bar{d} = (0, 0, -k_d, \tfrac{1}{2}is^{1/2})$, and putting all three nucleons on the mass shell, we obtain $q_0 = \tfrac{1}{2}s^{1/2}$, $k_d q_z = \tfrac{1}{4}(s - 2m_d^2)$, and $k_d^2 q_\perp^2 = -\tfrac{1}{4}m_N^2(s - s_d)$, where $s_d = 4m_d^2 - m_d^4 m_N^{-2}$. s_d is the well-known anomalous threshold associated with the deuteron form factor.

It is easy to generalize (8) and (11) to more general mass cases (Fig. 3). We shall always work in the c.m. frame of A and B (or C and D), with scattering taking place in the xz plane.

For Fig. 3(b), we define

$$Q_i = \tfrac{1}{2}[s^2 - s(m_A^2 + m_B^2 + m_E^2 + m_F^2) + (m_A^2 - m_B^2)(m_E^2 - m_F^2)]s^{-1} + m_G^2. \tag{12}$$

Then

$$k_i^2 q_\perp^{i2} = -\tfrac{1}{4}m_G^2(s - s_t^i)(s - s_{t'}^i)s^{-1}, \tag{13}$$

by making use of

$$Q_i^2 - 4k_i^2 |\vec{q}|^2 = m_G^2(s - s_t^i)(s - s_{t'}^i)s^{-1},$$

where $p_1 = (0, 0, k_i, iE_A^i)$, $E_A^{i2} = k_i^2 + m_A^2$, etc. The subscript or superscript i denotes that A and B are moving along the z direction.

For Fig. 3(c), we instead choose C and D along the z axis (and distinguish it by an index f). Then

$$k_f^2 q_\perp^{f2} = -\tfrac{1}{4}m_H^2(s - s_t^f)(s - s_{t'}^f)s^{-1}, \tag{14}$$

$p_2 = (0, 0, k_f, iE_c^f)$, etc., as one has an equal Q_f obtainable from Q_i by the substitution $(m_A, m_B, m_G) \to (m_C, m_D, m_H)$.

Finally, for Fig. 3(a), we obtain in either frame

$$4k_i^2 k_f^2 \sin^2\theta \, q_y^2 = 4k_i^2 k_f^2 |\vec{q}|^2 \sin^2\theta + 2Q_i Q_f k_i k_f \cos\theta - k_i^2 Q_f^2 - k_f^2 Q_i^2$$

$$= -\tfrac{1}{4}(t - t_n)(t - t_{n'})(s - s_b)(s - s_{b'})s^{-1}$$
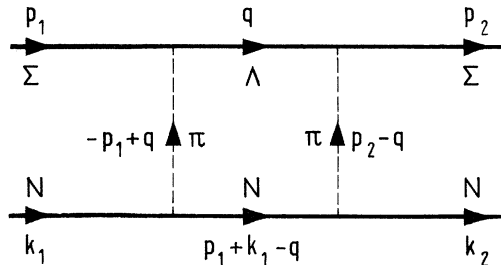
$$= -\tfrac{1}{4}K(s, t)s^{-1}, \tag{15}$$

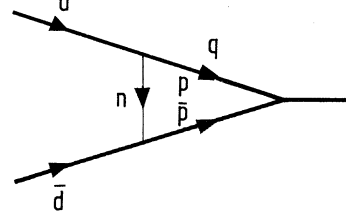FIG. 1. Box diagram possessing both triangular and box anomalous thresholds in the physical sheet.

FIG. 2. Deuteron triangle diagram.

where

$$(t - t_n)(t - t_{n'}) = t^2 - 2t(m_G{}^2 + m_H{}^2) + (m_G{}^2 - m_H{}^2)^2, \tag{16}$$

$$K(s,t) = 16 \begin{vmatrix} q^2 & p_1 \cdot q & k_1 \cdot q & p_2 \cdot q \\ p_1 \cdot q & p_1{}^2 & p_1 \cdot k_1 & p_1 \cdot p_2 \\ k_1 \cdot q & p_1 \cdot k_1 & k_1{}^2 & k_1 \cdot p_2 \\ p_2 \cdot q & p_1 \cdot p_2 & k_1 \cdot p_2 & p_2{}^2 \end{vmatrix}. \tag{17}$$

Whether $s_t{}^i$, $s_t{}^f$, and s_b of this general diagram show up in the physical sheet or not depends on the usual criterion that

$$m_F(m_E{}^2 + m_G{}^2 - m_A{}^2) + m_E(m_F{}^2 + m_G{}^2 - m_B{}^2) < 0, \quad m_F(m_E{}^2 + m_H{}^2 - m_C{}^2) + m_E(m_F{}^2 + m_H{}^2 - m_D{}^2) < 0,$$

and both conditions are satisfied or not, respectively. (13), (14), and (15) do not depend on these conditions, however.

Thus, in the first octant of a three-dimensional $|q_x| - |q_y| - |q_z|$ space (Fig. 4, which is a kind of "phase space" allowed for the vector $|\vec{q}|$), among all allowed configuration of $(|q_x|, |q_y|, |q_z|)$, s_n is a singular point located at the origin (fixed), s_t is another singular point sitting (somewhere) along the z axis (a function of the external masses), while s_b is another singularity lying (somewhere) in the xz plane (a function of t and the external masses). Since $|\vec{q}|^2$ is negative below the

normal threshold, $q_x{}^2$, $q_y{}^2$, and $q_z{}^2$ are not necessarily all positive definite. Thus s_b (corresponding to $|\vec{q}|^2 = q_x{}^2 + q_z{}^2$) can be greater than, equal to, or less than s_t (corresponding to $|\vec{q}|^2 = q_z{}^2$), depending on the value of t. Also, depending on the external masses, s_n, s_t, and s_b can coincide with each other.

It should be interesting to see if in nature $s_b > s_t$ when these singularities can be promoted above s_n. It should also be interesting to try a parametrization in terms of the relevant variables ($q_\perp{}^2$ or $q_y{}^2$) in the neighborhood of an anomalous threshold, should there be any observable effects associated with these singularities.

The author is indebted to Professor J. J. de Swart for a suggestion to investigate the anomalous thresholds in hyperon-nucleon scattering, which led to the plausible kinematical interpretation for these singularities given above. He also acknowledges useful communications with Professor R. Blankenbecler of the Stanford Linear
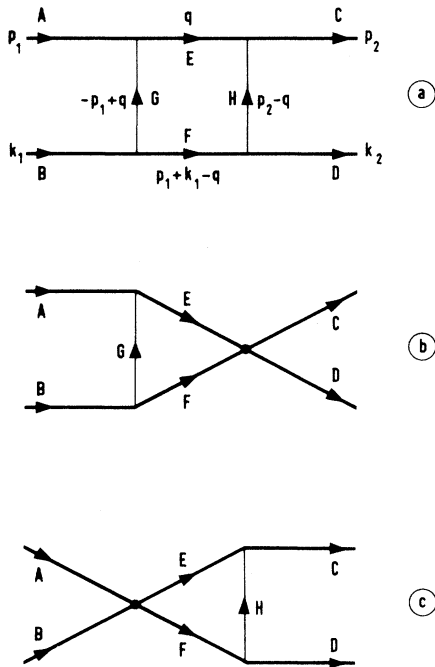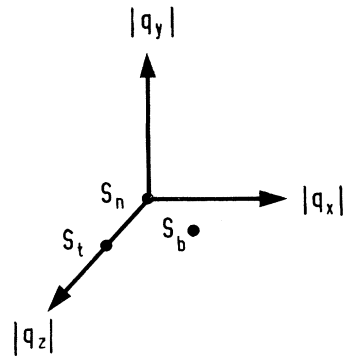

FIG. 3. General-mass box diagrams.

FIG. 4. "Phase-space" and the positions of the normal (s_n), triangular (s_t), and box (s_b) thresholds.

Accelerator Laboratory and Dr. J. S. Frederiksen of the University of Groningen.

[1]R. Karplus et al., Phys. Rev. 111, 1187 (1958).

[2]Y. Nambu, Nuovo Cimento 9, 610 (1958).

[3]R. Karplus et al., Phys. Rev. 114, 376 (1959).

[4]L. D. Landau, Nucl. Phys. 13, 181 (1959).

[5]R. E. Cutkosky, J. Math. Phys. (N.Y.) 1, 429 (1960).

[6]Here p stands for picking up the proper root of q_{i0} in performing the q_0 (loop energy) intergration [cf. M. T. Grisaru, Phys. Rev. 111, 1719 (1958), except for a numerical factor].

[7]S. Mandelstam, Phys. Rev. Lett. 4, 84 (1960).

[8]For examples, V. N. Gribov et al., Zh. Eksp. Teor. Fiz. 41, 924 (1961) [Sov. Phys. JETP 14, 659 (1962)]; K. Nishijima, Phys. Rev. 126, 852 (1962); J. S. Frederiksen and W. S. Woolcock, Australian National University Report (unpublished); Y. C. Liu and J. J. de Swart, to be published; etc.

[9]For examples, R. Oehme, Nuovo Cimento 13, 778 (1959); L. S. Liu, Phys. Rev. 125, 761 (1962); a review article by R. E. Cutkosky, Rev. Mod. Phys. 33, 448 (1961); etc.

[10]P. Collas and R. E. Norton, Phys. Rev. 160, 1346 (1967), and the references cited therein.

[11]$s = -(p_1 + k_1)^2 = (E_\Sigma + E_N)^2$, $t = -(p_1 - p_2)^2 = -2k^2(1 - \cos\theta)$, and the factors $-i\epsilon$ are omitted.

[12]Or $2\pi i\, \delta_p[(p_2 - q)^2 + m^2_\pi)]$ for $[(p_2 - q)^2 + m^2_\pi]^{-1}$ which has the same s_t and same discontinuity.

Origin of Magnetic Fields in the Early Universe

E. R. Harrison

Department of Physics and Astronomy, University of Massachusetts, Amherst, Massachusetts 01002

(Received 4 December 1972)

Primordial turbulence in the radiation era generates a weak seed magnetic field on all scales of the turbulence. This field is stochastically amplified by turbulence motions, and it is possible for magnetic and small-scale kinetic energies to attain equipartition within an expansion time. Field generation ceases at the epoch of equal radiation and matter densities, when the field strength is of the order of 1 G. It is estimated that the present intergalactic magnetic field has an intensity of $\sim 10^{-8}$ G and a scale-length of ~ 1 Mparsec.

An initially chaotic universe possesses many attractive features.[1] In particular, the chaotic inhomogeneities that survive in the extreme early universe will, quite probably, generate later a state of primordial turbulence in the radiation era. The significance and importance of primordial turbulence in galaxy formation, first stressed by von Weizsäcker[2] and Gamow,[3] has been investigated and discussed by many authors.[4] It has also been proposed that turbulence generates relatively intense magnetic fields during the radiation era of the early universe.[5]

The radiation era, in which blackbody radiation is more dense than matter, extends from $t \sim 10$ sec to $t \sim 10^5$ yr, where t is the Friedmann age. It is shown[6] that uniform rotation in this era generates the weak magnetic field

$$\vec{B} = -\alpha\vec{\zeta} = -2 \times 10^{-4}\vec{\zeta}\text{ G}, \tag{1}$$

where $\vec{\zeta}$ is the vorticity, and $\alpha = e/m_H c$ for a hydrogen plasma. From the ion equation of motion we obtain[7]

$$(d/dt)[R^2(\vec{\zeta}_i + \alpha\vec{B})] = R^2(\vec{\zeta}_i + \alpha\vec{B}) \cdot \nabla\vec{v}_i, \tag{2}$$

in which $d/dt = \partial/\partial t + (\vec{u} + \vec{v}) \cdot \nabla$ follows the motion; $\nabla \times \vec{v} = \vec{\zeta}$, where $\vec{v}$ is the subsonic turbulence velocity; and $\nabla \cdot \vec{u} = 3\dot{R}/R$, where $\vec{u}$ is the expansion velocity and $R(t)$ is the scaling variable. Hence, if the rotation were uniform, then

$$\vec{\zeta}_i + \alpha\vec{B} = \vec{\zeta}_1(R_1/R)^2, \tag{3}$$

where subscript 1 denotes initial values and $\vec{B}_1 = 0$. In a radiation-dominated plasma the electron and photon gases are tightly coupled by Thomson scattering and their vorticity $\vec{\zeta}$ varies as R^{-1}. The magnetic field of (3) is therefore generated in order to maintain $\vec{\zeta}_i \simeq \vec{\zeta}$ thus giving (1) when $R \gg R_1$.

The term on the right-hand side of (2) is responsible for stretching and winding field lines when rotation is nonuniform. Consequently, in a turbulent radiation era, a seed magnetic field on the order of magnitude of (1) is generated on all scales of the turbulence, and is then acted on and amplified stochastically by turbulence motions.

The ultimate state of an initially weak mag-